Carbon Microelectrodes with a Renewable Surface

Pavel Takmakov[a], **Matthew K. Zachek**[b], **Richard B. Keithley**[a], **Paul L. Walsh**[a], **Carrie Donley**[c], **Gregory S. McCarty**[b], and **R. Mark Wightman**[a],[*]

[a] Department of Chemistry, University of North Carolina at Chapel Hill, Chapel Hill, NC 27599, United States

[b] Department of Biomedical Engineering, University of North Carolina at Chapel Hill, North Carolina State University, Raleigh, NC 27607, United States

[c] Chapel Hill Analytical and Nanofabrication Laboratory, University of North Carolina at Chapel Hill, Chapel Hill, NC 27599, United States

Abstract

Electrode fouling decreases sensitivity and can be a substantial limitation in electrochemical experiments. In this work we describe an electrochemical procedure that constantly renews the surface of a carbon microelectrode using periodic triangle voltage excursions to an extended anodic potential at a scan rate of $400\ \mathrm{Vs}^{-1}$. This methodology allows for the regeneration of an electrochemically active surface and restores electrode sensitivity degraded by irreversible adsorption of chemical species. We show that repeated voltammetric sweeps to moderate potentials in aqueous solution causes oxidative etching of carbon thereby constantly renewing the electrochemically active surface. Oxidative etching was established by tracking surface-localized fluorine atoms with XPS, by monitoring changes in carbon surface morphology with AFM on pyrolyzed photoresist films, and also by optical and electron microscopy. The use of waveforms with extended anodic potentials showed substantial increases in sensitivity towards the detection of catechols. This enhancement arose from the adsorption of the catechol moiety that could be maintained with a constant regeneration of the electrode surface. We also demonstrate that application of the extended waveform could restore the sensitivity of carbon microelectrodes diminished by irreversible adsorption (electrode fouling) of byproducts resulting from the electrooxidation and polymerization of tyramine. Overall, this work brings new insight into the factors that affect electrochemical processes at carbon electrodes and provides a simple method to remove or reduce fouling problems associated with many electrochemical experiments.

Keywords

electrode fouling; carbon-fiber microelectrode; pyrolyzed photoresist film; dopamine; catechols; adsorption

INTRODUCTION

Carbon electrodes have several beneficial properties including a wide positive potential window, simplicity of surface modifications, and low cost [1,2]. These benefits have allowed applications of carbon electrodes in energy sources [3] and electroanalytical detection [4]. Recent progress in the development of nanostructured carbon for electrochemical sensors [5] and introduction of carbon based electronics [6] additionally highlight the important role of this

*CORRESPONDING AUTHOR: rmw@unc.edu.

material for a variety of future applications in both fundamental research and industrial processes.

Carbon microelectrodes are widely used in bioanalytical chemistry for the detection of neurotransmitters, signaling molecules, and their metabolites [4]. Due to their small size, microelectrodes can be used to probe chemical environments with high spatial resolution [7,8]. When coupled with fast scan cyclic voltammetry (FSCV), carbon fiber microelectrodes are capable of detecting and resolving analytes in real time. This technique has proven to be a valuable tool for providing a relationship between neurotransmitter release in the brain and animal behavior, which helps to establish functionality of several neurocircuits, particularly the dopaminergic system responsible for reward seeking behavior and learning [9,10]. Carbon electrodes have been shown to be much superior to other electrodes for this type of *in vivo* measurement [11].

Different treatments have been employed to increase adsorption and electron-transfer kinetics at carbon electrodes because these factors influence sensitivity, selectivity and response time. Physical treatments include traditional electrode polishing (glassy carbon) [2], vacuum heat treatment (glassy carbon) [12], laser activation of electrode surfaces (glassy carbon) [13] and flame etching (carbon fibers) [14]. All produce changes in the structure of carbon surfaces that lead to the desired electrochemical response. Despite the success of these physical pretreatments for achieving particular electrode properties, these approaches have several disadvantages. First, it is difficult to predict electrode performance when comparing different pretreatment methodologies on different forms of carbon. McCreery and coworkers have developed a relationship between carbon electrode surface structure and electron-transfer kinetics [15], however this paradigm does not consider adsorption that plays an important role for the many electroactive analytes including catechols [16,17]. A second limitation is that these surfaces cannot be renewed once implanted within a biological system. This is particularly important for *in vivo* voltammetry since it is difficult to repeat the sensitivity enhancing treatment step during the biological experiment. Thus, the reported procedures have limited applicability for *in vivo* work particularly for experiments with freely moving animals.

Another pretreatment approach that has proven to be useful is electrochemical oxidation of carbon. Oxidation of carbon fibers with a DC potential of 2.5 V leads to an electrode with a greatly increased capacitance due to fracturing of the fiber [18]. This treatment is reported to increase the amount of oxides on the fiber surface [19]. Oxidation of carbon fibers with a triangular waveform extended to 3 V (repeated at 70 Hz) irreversibly alters their electrochemical response [20,21]. Electron-transfer kinetics are accelerated for many species and adsorption is greatly enhanced [22]. Repetitive FSCV at carbon-fiber microelectrodes with a potential limit of 1.4 V vs Ag/AgCl has been shown to increase adsorption when compared to the use of potential limit of 1.0 V while maintaining current stability both *in vitro* and *in vivo*[23,24]. Increased adsorption enhances sensitivity but, at the same time, the background amplitude is also increased. This treatment differs from others in that the waveform is continually applied during the analytical measurement. However, the mechanisms behind this enhancement with extended voltage scans are unknown.

The small size of carbon-fiber microelectrodes limits the surface analysis techniques that can be used to investigate chemical changes on the carbon surface. In this work we have used pyrolyzed photoresist film (PPF) carbon electrodes to investigate the underlying changes that arise with increased positive limits during repetitive scans. PPF films have similar electrochemical properties as carbon-fiber microelectrodes but can be patterned into a variety of shapes using microfabrication techniques [25–28]. These carbon surfaces were probed with X-ray photoelectron spectroscopy (XPS) and atomic force microscopy (AFM). Our findings

indicate that the surface of these electrodes is constantly renewed by using periodic application of waveforms with an extended anodic potential.

EXPERIMENTAL SECTION

Chemicals

All chemicals were obtained from Sigma-Aldrich (St. Louis, MO, USA) unless otherwise noted and used as received. Solutions were prepared using doubly distilled water. Electrochemical experiments were done in PBS buffer (140 mM NaCl, 3 mM KCl, 10 mM NaH_2PO_4, pH = 7.4). Stock solutions of catechols were prepared in 0.1 N $HClO_4$ and diluted to the desired concentration immediately before use.

Fabrication of Carbon Fiber Microelectrodes

Cylindrical microelectrodes were constructed using a T-650 carbon fiber (Thornel, Amoco Corp., Greenville, SC, USA) as previously described [29]. Briefly, individual carbon fibers were aspirated into glass capillaries (A-M Systems, Carlsborg, WA, USA) using vacuum. Afterwards, the capillaries were pulled and sealed with a micropipette puller (Narishige, Tokyo, Japan). The quality of the pulled capillaries was examined with an optical microscope. The carbon fibers were cut to an exposed length of 100 μm. Before electrochemical experiments, electrodes were soaked in isopropanol purified with Norit A activated carbon (ICN, Costa Mesa, CA, USA) for at least 20 min to remove surface impurities [17]. Electrical connection to the carbon fiber was made with electrolyte (4 M CH_3COOK and 0.15 M KCl), and a stainless steel wire.

Fabrication of PPF Electrodes

Two types of PPF microelectrodes that differed in their insulation were fabricated. SU-8 insulated PPF electrodes were used for studies of background current change with electrochemical treatment and silicon nitride insulated PPF electrodes were used for XPS and AFM studies. The PPF microelectrodes were fabricated as described previously [28]. Briefly, photoresist (AZ1518, AZ Electric Materials, Branchburg, NJ, USA) was spun on a 3″ fused silica wafer and patterned using standard photolithographic techniques. The patterned wafer was subsequently pyrolyzed at 1000 °C under a forming gas atmosphere (5% H_2, 95% N_2). A microprocessor controlled tube furnace (Sentro Tech, Inc., Berea, OH, USA) was used to ramp the temperature at 5 °C/min and it was held at 1000 °C for one hour. Samples were allowed to cool to room temperature under the forming gas atmosphere prior to exposure to air.

To obtain contrast for XPS mapping studies a non-carbon dielectric was required. For this application, a Si_3N_4 layer deposited by plasma-enhanced chemical vapor deposition (PECVD) was used to insulate the PPF microelectrodes. The Si_3N_4 films were deposited using an Advanced Vacuum Vision 310 PECVD System (Lomma, Sweden). Monosilane (2% SiH_4/N_2) and ammonia (NH_3) gases were used at electronically mass controlled flow rates. The films were deposited at a rate of 7.5 nm/min to a final thickness of 500 nm. The exposed microelectrode area was photolithographically defined, and subsequently etched using reactive ion etching (Semi Group Inc, USA) under a fluoroform (CHF_3) and oxygen atmosphere. The pyrolyzed carbon served as a sufficient etch stop for this process. All deposition and etch rates were determined using a Tencor, P-6 profilometer (KLA-Tencor Inc, Milpitas, CA, USA). To obtain non-roughened and non-fluorinated samples, PPF microelectrodes were insulated with SU-8 3010, as previously reported [28]. External connections to the PPF were made using silver epoxy (MG Chemicals, Burlington, Ontario, Canada) and stainless steel wires. The device was cut with a dicing saw into its final form that had four PPF electrodes, each of which was 75 μm by 100 μm. Electrodes with such areas are compatible with small spot XPS measurements with a 27 μm diameter.

Electrochemical Experiments

Cyclic voltammograms were acquired with an EI-400 potentiostat used in two electrode mode and TH-1 software (ESA Inc, Chemsfold, MA, USA) written in LabVIEW (National Instruments, Austin, TX, USA). The waveform was generated and the voltammetric signal was acquired with an ADC/DAC card PCI-6251 (National Instruments). A PCI-6711 DAC board (National Instruments) was used to synchronize waveform application, data acquisition and TTL pulses for the flow injection valve. The output waveform was filtered with a low pass 2 kHz filter to eliminate digitization steps.

For electrochemical measurements, three triangular waveforms were used. The first waveform (referred to as the 1.0 V waveform) was a ramp from −0.4 V to 1.0 V and back to −0.4 V at a scan rate of 300 Vs^{-1} repeated at 10 Hz with a rest potential of −0.4 V between scans. A second waveform (referred to as the 1.3 V waveform) was a ramp from −0.4 V to 1.3 V and back to −0.4 V at scan rate of 400 Vs^{-1} repeated at 60 Hz, also with a rest potential of −0.4 V between scans. The third waveform (referred to as the 1.4 V waveform) was a ramp from −0.6 to 1.4 V and back to −0.6 V at scan rate of 400 Vs^{-1} repeated at 60 Hz with a rest potential of −0.6 V between scans. The latter two extended waveforms were applied at a frequency of 60 Hz to intensify any oxidative etching effects and to reduce the duration of the electrochemical experiments. In each experiment background current was allowed to stabilize for 15 minutes [24].

Evaluation of the adsorption of catechols employed the same waveforms but with a repetition frequency of 1 Hz. The charge was obtained by integrating the oxidation peak of the cyclic voltammogram as previously described [17]. The area of the electrode was calculated from microelectrode dimensions measured with an optical microscope. To account for contributions from diffusion, cyclic voltammograms were simulated with DigiSim software (Bioanalytical Systems Inc, West Lafayette, IN, USA) using kinetic parameters and diffusion coefficients reported before [30,31]. The amount of adsorbed analyte was obtained by subtracting the computed diffusional component from the measured charge and converting it to the number of moles using Faraday's law.

For tyramine fouling experiments, the carbon fiber microelectrode was cycled for 15 minutes in buffer with the 1.3 V waveform at 60 Hz. The response to 500 nM dopamine in a flow injection system was monitored for 10 consecutive injections 3 minutes apart using the 1.0 V waveform for detection (10 Hz application frequency). Then, the electrode was purposely fouled by applying the 1.0 V waveform at 10 Hz in 15 mM solution of tyramine in PBS buffer for 15 minutes. Afterwards, the response to 500 nM dopamine was again evaluated with the 1.0 V waveform for 10 consecutive injections 3 minutes apart (10 Hz application frequency). The recovery of electrode sensitivity was evaluated by cycling the electrode with the 1.3 V waveform in PBS buffer for 15 minutes at 60 Hz followed by testing with 500 nM dopamine in the flow-injection system with the 1.0 waveform for 10 consecutive injections 3 minutes apart (10 Hz application frequency). The responses for the 10 consecutive injections for each condition were averaged and normalized to the pre-tyramine injections.

All potentials are reported versus a Ag/AgCl reference electrode. Electrochemical measurements were performed in a grounded Faraday cage.

Flow Injection Apparatus

The flow injection analysis system consisted of a syringe pump (Harvard Apparatus, Holliston, MA) that directed buffer solution through a Teflon tube to a 6-port injection valve (Rheodyne, Rohnert Park, CA, USA) at rate of 0.5 mL per minute. The injection valve was controlled by a 12 V DC solenoid and was used to introduce analyte from an injection loop (volume of 0.7

mL) into an electrochemical cell. The carbon-fiber microelectrode was placed inside the opening of the Teflon tube to eliminate the diffusion broadening and a reference electrode was placed within ~ 20 mm of the working electrode [32].

Electrochemical Modification of PPF Electrodes

Electrochemical experiments involving PPF microelectrodes were accomplished using a drop of buffer placed on top of the microelectrodes and a reference electrode was lowered into the buffer. The three different waveforms were applied to separate electrodes for 30 minutes. Electrodes were rinsed with water, dried in air and the surface was analyzed with XPS and AFM.

XPS Analysis

Drops of saturated NiI_2 solution were deposited onto the four corners surrounding each of the electrodes using a pressure ejection to help locate the PPF microelectrode during XPS analysis. Glass capillaries with a 0.68 mm inner diameter (AM Systems, Sequim, WA, USA) were pulled on a Sachs-Flaming Micropipette Puller Model PC-84 (Sutter Instruments, Novato, CA, USA) and bumped to a final inner diameter of 10–15 μm at the tip. Approximately 20–30 μm diameter droplets were then deposited onto the substrate under an inverted microscope Nikon Eclipse TE 300 (Nikon, Lewisville, TX, USA) at 5–10 psi for 10–100 ms using a Picospritzer (Parker Instruments, Pine Brook, NJ, USA). The solution was then allowed to evaporate for approximately 15 minutes in a 100 °C oven.

To investigate the chemical composition of the native PPF surface, a separate sample was prepared. A cooled wafer with a carbon film was transferred from the furnace to the XPS instrument in a desiccator under N_2 to minimize oxidation by atmospheric oxygen and to record the XPS spectra of a freshly prepared PPF surface. No subsequent insulation steps were done for this sample.

XPS analysis was performed with a Kratos Axis Ultra DLD X-ray Photoelectron Spectrometer (Kratos Analytical Inc, Chestnut Ridge, NY, USA) using a monochromatic Al K_α x-ray source. The surface was mapped for the Si 2p and Ni $2p_{3/2}$ lines to spatially locate the electrode. Spectra were taken from the center of the electrode with a sampling area with diameter of 27 μm.

AFM Imaging

AFM images were obtained with a MFP3D Atomic Force Microscope (Asylum Research, Santa Barbara, CA, USA) in tapping mode. After the various electrochemical modifications of PPF electrodes, the surface was examined in 5 μm by 5 μm areas. The sampling spots were randomly chosen from different locations of the PPF electrode to ensure representative sampling and averaging. The roughness for each sample was calculated for several 1 μm by 1 μm spots in Igor Pro 6.1 (WaveMetrics Inc, Lake Oswego, OR, USA). AFM data were plotted using ARgyle Light software (Asylum Research, Santa Barbara, CA, USA).

Scanning Electron Microscopy

Carbon-fiber microelectrodes were imaged before and after electrochemical treatment with an FEI Quanta 200 FEG environmental scanning electron microscope (FEI Company, Hillsboro, OR, USA).

Optical Microscopy

Etched PPF microelectrodes were imaged with Nikon Eclipse TE 300 inverted microscope (Nikon, Lewisville, TX, USA). Pictures were taken with Nikon digital camera. Etched carbon-fiber microelectrodes were photographed with an IR-1000 infrared CCD monochrome video

camera (DAGE-MTI, Michigan City, IN) fixed to a Nikon FN-S2N upright microscope and collected with Video Advantage ® ADX PCI card and software (Turtle Beach, Elmsford, NY). Images were processed using Adobe Photoshop (Adobe Systems Inc, San Jose, CA, USA).

Data Analysis

For adsorption studies, cyclic voltammograms for catechols were background subtracted, digitally filtered and averaged using TH-1 software (ESA Inc, Chemsfold, MA, USA) using previously reported methodology [17]. XPS data for loss of fluorine was analyzed with a one-way ANOVA with Dunnett's post test using GraphPad Prism (GraphPad Software, San Diego, CA, USA). SEM images were processed using ImageJ (Rasband, W.S., ImageJ, National Institutes of Health, Bethesda, MD, USA). Statistical analysis of the data and generation of the plots were done using MS Excel and GraphPad Prism. All numbers are reported as averages ± standard deviation.

RESULTS AND DISCUSSION

Effect of Applied Potential on Background Current of Carbon Microelectrodes

Due to its small size and geometry, the surface chemistry of the carbon-fiber microelectrode is difficult to study with modern surface-analysis techniques. To circumvent this problem, we used PPF electrodes that are more amenable to AFM and XPS analysis. PPF has been shown to be structurally similar to glassy carbon [26]. Like carbon-fiber microelectrodes, PPF was previously reported to have similar increases in sensitivity towards dopamine when extended waveforms were used with FSCV [28]. The area of the PPF electrodes in this work was 7500 μm^2 which is 7–8 times larger than the area of a 100 μm long cylindrical carbon-fiber microelectrode (~ 1000 μm^2). This area was selected as a compromise so that *iR* drop was only slightly greater than that of carbon-fiber microelectrodes but so that there was sufficient area for surface analysis.

The high scan rates used in FSCV induce large background currents at carbon electrodes that originate from charging of the electrode double layer [33] and oxidation and reduction of electrochemically active surface groups [34,35]. The background current is linearly proportional to the scan rate and electrode area. Application of the extended waveforms led to increases in background currents on carbon-fiber microelectrodes (Figure 1A–C). Similarly, cycling of PPF electrodes over 15 minutes with the 1.3 V waveform (Figure 1E and H) and with the 1.4 V waveform (Figure 1F and I) increased the background current but cycling with 1.0 V waveform did not lead to any change (Figure 1D and G). The increase in the background current for the extended waveforms compared with the 1.0 V waveform was more pronounced for PPF electrodes. The possible reason for this observation is the fact that initially PPF is mostly hydrogen terminated with only a small amount of surface oxygen groups [27,36]. We hypothesize that this renders the microelectrode surface hydrophobic and unwettable. In turn, this unwettable surface repels the electrolyte solution and reduces the capacitance of the double layer which leads to a decreased background current.

As the potential limit is made more positive, the current at the most positive potential shows a slight increase at both PPF and carbon-fiber electrodes. This feature has been previously assumed to arise from oxidation of carbon at these positive potentials [24]. Such a process could increase the amount of oxides on the carbon surface and could cause a loss of electrode mass as is found when passing current through bundles of carbon fibers to generate carbon dioxide [37]. Indeed, overoxidation of highly ordered pyrolyzed graphite (HOPG) induces the formation of blisters on the surface of HOPG presumably due to evolution of carbon dioxide [38]. Besides formation of CO_2, oxidation of carbon surfaces has been shown to cause exfoliation of carbon either as graphite oxide as was suggested to occur during the blistering of HOPG [38] or as carbon

particles or nanocrystals [39–41]. These observations imply that scanning to the higher potentials might change the surface of carbon electrode. Surface analysis techniques were used to establish the occurrence of these processes on the carbon surface with the electrochemical treatment.

Characterization of Surface Effects of Potential Cycling on PPF Electrodes

XPS was used to sample the elemental composition of PPF electrode surfaces. For a sample prepared without insulation and stored in a desiccator to prevent oxidation by atmospheric oxygen, XPS showed approximately 5% surface oxygen (Figure 2A), a value similar to that previously reported [26,27]. Subsequent deposition of the Si_3N_4 insulation followed by etching with a fluoroform/oxygen plasma introduced a fluorine marker on the surface (F/C atomic ratio of 0.15 ± 0.09, Figure 2B). The deposition of fluorine on the surface after treatment with fluoroform/oxygen plasma has been previously reported [42]. Cycling the electrodes with either the 1.3 V (F/C ratio of 0.008 ± 0.008, Figure 2C) or the 1.4 V (Figure 2D, fluorine was not detected) waveforms for 30 minutes removed fluorine from the surface in a manner that depends on the maximum applied potential (summarized Figure 2E). In contrast, potential scans to 1.0 V do not result in the removal of the fluorine marker (data not shown). These results indicate that the fluorine introduced on the surface during the Si_3N_4 etching is removed by cycling the electrode to the more positive potentials of 1.3 or 1.4 V. The surface oxygen content also increased to $21 \pm 8\%$ after treatment with both 1.3 V and 1.4 V waveforms.

Physical Changes Caused by Electrochemical Potential Limits

The roughness of the PPF electrodes used in this work was established with AFM. The roughness of a freshly prepared PPF surface was comparable to the roughness of the fused silica substrate (Figure 3A) with a RMS roughness of 0.45 ± 0.03 nm vs 0.94 ± 0.06 nm for the fused silica substrate (data not shown). However, when the PPF was coated with silicon nitride, and the insulator was subsequently etched and removed with a fluoroform/oxygen plasma, the resulting PPF surface showed a considerable increase in roughness (RMS 18 ± 5 nm, Figure 3B). The formation of rough features on the carbon surface was caused by the fluoroform/oxygen plasma used for Si_3N_4 removal that has been reported to slowly etch carbon [42].

Surface roughness was also evaluated after electrochemical scanning. Application of the 1.3 V waveform at 60 Hz for 30 min caused a decrease in the surface roughness (RMS 9 ± 5 nm, Figure 3C) compared to the surface after etching. Smoothing of the carbon surface was even more pronounced with the 1.4 V waveform (RMS 5 ± 3 nm, Figure 3D). The difference in etching rates between the two extended waveforms is consistent with the XPS data for fluorine tracking where the larger overpotential caused more substantial removal of fluorine. Figure 3E graphically illustrates the change in surface roughness for different treatments. Repetitive scanning to 1.0 V did not alter the surface roughness (data not shown).

The AFM data revealed that the topography of fluoroform/oxygen plasma treated PPF electrodes before electrochemical treatment have peak-to-valley roughness values on the scale of 80 nm per 5 μm of lateral length. Application of the extended waveforms for 30 minutes led to the formation of a surface with 10–20 nm peak-to-valley change in height per 5 μm of lateral length. These results suggest that complete etching of a PPF electrode with a thickness of 400 nm could be accomplished within hours with these electrochemical treatments.

This hypothesis was verified by examining the electrode after multiple scans. During scanning the background current was monitored using both the 1.3 V and 1.4 V waveforms. The use of the PPF electrodes with the 1.3 V waveform applied at 60 Hz led to a decrease in the background within 10 hours and a similar disappearance of the background with the 1.4 V waveform after

1.5 hours. After the disappearance of the background, optical microscopy was used to examine the PPF microelectrodes. In both cases, the PPF electrodes had disappeared (Figure 4C, D). The electrodes did not disappear if they were immersed in the buffer solution (Figure 4B) for a similar time period without potential control or when they were scanned repetitively to 1.0 V. From the thickness of the PPF layer (400 nm), an estimate of the time for electrode disintegration can be established from the decrease in the background current. Etching rates were estimated to be 0.7 nm/min for the 1.3 V waveform and 4.4 nm/min for the 1.4 V waveform, both repeated at 60 Hz. The roughness of these electrodes is not directly responsible for the etching because complete electrode dissolution within similar time frames was also observed for SU-8 insulated PPF electrodes (data not shown).

Do the waveforms with extended anodic potentials cause etching of only PPF electrodes, or do they affect other forms of carbon as well? PAN-type carbon fibers were used as a comparison. Carbon-fiber microelectrodes are routinely used for voltammetric detection of catecholamines both *in vitro* and *in vivo*. The diameter of the most popular carbon fibers (T-650) used in these types of experiments is 5 μm. If etching takes place on a carbon-fiber microelectrode, then it should be possible to observe the change in carbon-fiber diameter with optical or electron microscopy. As a control experiment, the 1.0 V waveform was applied at 60 Hz for 65 hours; it showed no significant change in carbon fiber diameter (compare Figure 5A and 5B). However, prolonged application of the 1.3 V waveform at 60 Hz led to complete etching of the carbon-fiber microelectrode within 65 hours (Figure 5C). Application of the 1.4 V waveform led to a much faster etch rate causing the complete dissolution of the carbon fiber within just 6 hours (Figure 5D). For complete etching of the carbon fiber within 6 hours as seen with the 1.4 V waveform, the etching rate would be 7.5 nm/min, in the same range as observed at PPF electrodes.

Electron microscopy revealed in greater detail the oxidative etching-induced changes of the carbon fiber (Figure 5E and Figure 5F). The average decrease in diameter of the carbon fibers was 0.9 ± 0.4 μm (n = 4) after 30 hour treatment with the 1.3 V waveform. Thus, application of the 1.3 V waveform to the carbon-fiber microelectrode produced a linear etch rate of 0.24 ± 0.11 nm/min, which is smaller than the etch rate observed for PPF electrodes.

The etching of the carbon fibers also takes place with the extended waveforms applied at lower frequencies. Complete etching of carbon fibers was observed after 36 hours of application of the 1.4 V waveform at 10 Hz. This was achieved after 1.3×10^6 potential cycles with the 1.4 V waveform and after 1.4×10^7 potential cycles with the 1.3 V waveform. Thus, the oxidative etching rate is linearly proportional to the frequency of the applied waveform.

Increased Adsorption of Catecholamines Resulting from Oxidative Etching of Carbon Fiber Microelectrodes

Regeneration of a fresh electrode in real time is advantageous during many electrochemical experiments. The chief benefit of this electrochemical surface treatment is the consistency in the electrochemical properties of carbon electrodes from experiment to experiment since the surface is renewed repeatedly. However, it is important to establish electrochemical performance of this surface towards redox active molecules. The kinetics and thermodynamics of electrochemical oxidation for catechols on carbon have been well documented [30], and the biological importance of these molecules as neurotransmitters and metabolites makes them the analyte of choice [7]. As previously established, catecholamines strongly adsorb to the carbon surface [16,17]. Many researchers utilize the extended waveforms because it has previously been reported to increase the adsorption of dopamine onto the electrode surface [24]. Catechols with different functional groups were used in this work to probe the nature of adsorption sites on the carbon at extended potential limits.

The use of the 1.3 V and 1.4 V waveforms significantly increased adsorption of positively charged dopamine (Figure 6A) with the 1.4 V waveform having the most pronounced effect. A lesser effect was observed for a neutral molecule, 4-methylcatechol (4MC) (Figure 6B). Again, the 1.4 V waveform demonstrated the greatest increase in adsorption. Adsorption of negatively charged 3,4-dihydroxyphenylacetic acid (DOPAC) was also promoted by the extended waveform (Figure 6C). Curiously, the surface coverage for both 4MC and DOPAC was almost identical for the 1.0 V waveform which suggests that the catechol moiety is responsible for the affinity of these molecules towards carbon. This effect was previously explained through a π- π stacking mechanism between the catechol benzene ring and the aromatic π- π system of the carbon electrode [43]. A similar increase in surface coverage was observed for 4MC and DOPAC with the use of the 1.3 V waveform. Adsorption of DOPAC for the 1.4 V waveform was almost identical to the 1.3 V waveform. The 1.4 V waveform has a more negative holding potential (−0.6 V) so electrostatic repulsion may be greater, hindering the adsorption of DOPAC as compared to the neutral 4MC. Overall, these data indicate that the use of extended waveforms generates a highly adsorptive surface for catechols that facilitates their detection. We hypothesize that this property can be attributed to constant regeneration of adsorption sites.

Previously, this increase in catecholamine adsorption was attributed to the formation of high affinity adsorption sites composed from surface oxides [24]. The oxides are thought to be introduced by the oxidation of carbon at higher anodic potentials, and this is supported by our observation of high O/C atomic ratios by XPS after scanning to 1.3 or 1.4 V. In previous reports the passing of a substantial amount of charge through bundles of carbon fibers has been shown also to result in a decrease in the mass of the electrode indicating that the oxidation of carbon-fiber surfaces leads to either evolution of carbon dioxide and its further dissolution in the liquid phase [37] or generation of graphite oxide [38] and carbon particles or nanocrystals [39–41]. Also electrochemical etching of carbon etching was reported before for bundles of carbon fibers [44], glassy carbon [45] and PPF[44], however in all these cases high DC potentials and high current densities were used in highly basic or acidic solutions that makes it difficult to use these methods for *in vivo* experiments.

Interestingly, the XPS study of oxidized carbon fiber bundles indicated formation of carboxylic and ester surface bond groups on the carbon after electrooxidation [37]. The carboxylic groups could act as high affinity binding sites for dopamine due to electrostatic interactions. The possibility of similar electrostatic interaction as the origin of increased adsorption was confirmed by previous work by Hermans et al [46]. In that case, the increase in adsorption of dopamine was observed after immobilization of negatively charged sulfonate groups on the carbon surface.

We hypothesize that the carbon overoxidation proceeds through the formation of carboxylic groups on the carbon surface with further oxidation through Kolbe-like electrolysis [47,48]. In this hypothesized reaction the oxidation of surface-confined carboxylic groups leads to the formation of carbon dioxide. The process can function in cyclical manner constantly generating carboxylic groups as well as consuming them by formation of CO_2. Our hypothesis implies that cyclic regeneration prevents fouling of active sites by the irreversible adsorption of impurities and products of oxidation of analytes.

Recovery of Fouled Carbon Microelectrodes by Overoxidative Surface Renewal

To test the hypothesis that the continuous etching of the carbon electrode with the use of extended waveforms regularly regenerates a fresh carbon surface, we purposefully fouled the carbon-fiber microelectrodes by electropolymerization of tyramine. The electrooxidation products of tyramine are known to polymerize and form an impermeable film on the electrode surface which deteriorates electrode sensitivity [49–51]. Carbon-fiber microelectrodes were first

treated with the 1.3 V waveform (60 Hz) for 15 minutes to generate a fresh and active surface. Subsequently, the response to 500 nM dopamine in a flow injection system with the 1.0 V waveform (10 Hz) was measured. This waveform was shown not to alter the carbon fiber surface (Figure 7A and Figure 7D, data for 3 microelectrodes pooled together). The sensitivity of the electrodes was 19 ± 4 nA for 500 nM dopamine. The microelectrodes were then passivated by immersing them in a 15 mM solution of tyramine, and the 1.0 V waveform (10 Hz) was applied to the electrode for 15 minutes. The electrodes were then tested for their sensitivity to dopamine and it was found that tyramine treatment decreased the sensitivity of the electrode to dopamine to 0.6 ± 0.4 nA or 3 % of its initial value. The cyclic voltammograms of dopamine were substantially distorted in shape (Figure 7B and Figure 7D). However, 15 minutes of cycling with the 1.3 V waveform almost completely restored sensitivity towards dopamine (Figure 7C and Figure 7D). These data demonstrate that the application of the extended waveform regenerates the electrode surface and creates new active sites for catecholamine adsorption. The surface cleaning induced by the extended waveform also confirms previously suggested activation of carbon surface if scanned to 1.4 V that facilitates oxidation of histamine on carbon-fiber microelectrode [52].

CONCLUSIONS

This work demonstrates that the use of the waveforms with extended anodic potentials for FSCV (up to 1.3 V and 1.4 V vs Ag/AgCl) at carbon electrodes causes oxidative etching of the surface, a process that is not detectable with similar scans to 1.0 V. PPF microelectrodes were used to establish the effect with the aid of surface analysis techniques (XPS and AFM). Both XPS and AFM tracking of surface integrity showed etching of the carbon electrode following the application of these waveforms. Exposure of PPF microelectrodes to the extended waveforms for long periods of time (up to 10 hours) led to complete etching of the electrodes, confirmed with optical microscopy. Oxidative etching was shown to occur on carbon-fiber microelectrodes with complete removal observed after 65 hours (for the 1.3 V waveform) or 6 hours (for the 1.4 V waveform). We postulate that the etching occurs as a consequence of evolution of carbon dioxide or exfoliation of graphite oxide and/or carbon particles take place. Oxidative etching of the carbon electrodes with the extended waveforms provides a number of benefits in electroanalytical detection.

The important result of oxidative etching is the continuous regeneration of a fresh carbon surface. The ability to renew electrode surfaces helps to prevent electrode fouling. The demonstrated effect maybe the reason why carbon-fiber microelectrodes remain active in vivo which makes a carbon microelectrode a useful analytical tool for the *in vivo* detection of catecholamines since the state of the surface can be restored by a simple electrochemical procedure. In addition, microelectrodes with a renewable surface open new horizons for the use of waveforms with extended anodic potential limits for the electrochemical detection in chemically complex environments since this continual surface regeneration prevents electrode fouling and maintenance of electrode sensitivity.

Acknowledgments

References

1. McCreery, RL. Carbon electrodes: structural effects on electron transfer kinetics. Vol. 17. Marcel-Dekker; New York: 1991.

2. Kissinger, PT.; Heineman, WR. Laboratory Techniques in Electroanalytical Chemistry. Marcel Dekker Inc; 1996.

3. Pandolfo AG, Hollenkamp AF. Journal of Power Sources 2006;157:11–27.

4. McCreery RL. Chemical Reviews 2008;108:2646–2687. [PubMed: 18557655]

5. Balasubramanian K, Burghard M. Analytical and Bioanalytical Chemistry 2006;385:452–468. [PubMed: 16568294]

6. Avouris P, Chen ZH, Perebeinos V. Nature Nanotechnology 2007;2:605–615.

7. Robinson DL, Hermans A, Seipel AT, Wightman RM. Chemical Reviews 2008;108:2554–2584. [PubMed: 18576692]

8. Kita JM, Wightman RM. Current Opinion in Chemical Biology 2008;12:491–496. [PubMed: 18675377]

9. Owesson-White CA, Cheer JF, Beyene M, Carelli RM, Wightman RM. Proceedings of the National Academy of Sciences of the United States of America 2008;105:11957–11962. [PubMed: 18689678]

10. Roitman MF, Wheeler RA, Wightman RM, Carelli RM. Nature Neuroscience 2008;11:1376–1377.

11. Zachek MK, Hermans A, Wightman RM, McCarty GS. Journal of Electroanalytical Chemistry 2008;614:113–120. [PubMed: 19319208]

12. Fagan DT, Hu IF, Kuwana T. Analytical Chemistry 1985;57:2759–2763.

13. Poon M, Mccreery RL. Analytical Chemistry 1986;58:2745–2750.

14. Strand AM, Venton BJ. Analytical Chemistry 2008;80:3708–3715. [PubMed: 18416534]

15. Chen PH, McCreery RL. Analytical Chemistry 1996;68:3958–3965.

16. Baur JE, Kristensen EW, May LJ, Wiedemann DJ, Wightman RM. Analytical Chemistry 1988;60:1268–1272. [PubMed: 3213946]

17. Bath BD, Michael DJ, Trafton BJ, Joseph JD, Runnels PL, Wightman RM. Analytical Chemistry 2000;72:5994–6002. [PubMed: 11140768]

18. Gotch AJ, Kelly RS, Kuwana T. Journal of Physical Chemistry B 2003;107:935–941.

19. Xie YM, Sherwood PMA. Chemistry of Materials 1990;2:293–299.

20. Gonon F, Buda M, Cespuglio R, Jouvet M, Pujol JF. Nature 1980;286:902–904. [PubMed: 7412872]

21. Gonon FG, Fombarlet CM, Buda MJ, Pujol JF. Analytical Chemistry 1981;53:1386–1389.

22. Kovach PM, Ewing AG, Wilson RL, Wightman RM. Journal of Neuroscience Methods 1984;10:215–227. [PubMed: 6738110]

23. Hafizi S, Kruk ZL, Stamford JA. Journal of Neuroscience Methods 1990;33:41–49. [PubMed: 2232859]

24. Heien MLAV, Phillips PEM, Stuber GD, Seipel AT, Wightman RM. Analyst 2003;128:1413–1419. [PubMed: 14737224]

25. Kim J, Song X, Kinoshita K, Madou M, White B. Journal of the Electrochemical Society 1998;145:2314–2319.

26. Ranganathan S, McCreery R, Majji SM, Madou M. Journal of the Electrochemical Society 2000;147:277–282.

27. Ranganathan S, McCreery RL. Analytical Chemistry 2001;73:893–900. [PubMed: 11289433]

28. Zachek MK, Takmakov P, Moody B, Wightman RM, McCarty GS. Analytical Chemistry 2009;81:6258–6265.

29. Cahill PS, Walker QD, Finnegan JM, Mickelson GE, Travis ER, Wightman RM. Analytical Chemistry 1996;68:3180–3186. [PubMed: 8797378]

30. Deakin MR, Wightman RM. Journal of Electroanalytical Chemistry 1986;206:167–177.

31. Gerhardt G, Adams RN. Analytical Chemistry 1982;54:2618–2620.

32. Kristensen EW, Wilson RL, Wightman RM. Analytical Chemistry 1986;58:986–988.

33. Bard, AJ.; Faulkner, LR. Electrochemical Methods. Wiley; New York: 2001.

34. Kawagoe KT, Garris PA, Wightman RM. Journal of Electroanalytical Chemistry 1993;359:193–207.

35. Runnels PL, Joseph JD, Logman MJ, Wightman RM. Analytical Chemistry 1999;71:2782–2789. [PubMed: 10424168]

36. Hermans, A. Ph D Thesis. University of North Carolina; Chapel Hill: 2007.

37. Yue ZR, Jiang W, Wang L, Gardner SD, Pittman CU. Carbon 1999;37:1785–1796.

38. Goss CA, Brumfield JC, Irene EA, Murray RW. Analytical Chemistry 1993;65:1378–1389.

39. Zhou JG, Booker C, Li RY, Zhou XT, Sham TK, Sun XL, Ding ZF. Journal of the American Chemical Society 2007;129:744–745. [PubMed: 17243794]

40. Lu J, Yang JX, Wang JZ, Lim AL, Wang S, Loh KP. ACS Nano 2009;3:2367–2375. [PubMed: 19702326]

41. Zheng LY, Chi YW, Dong YQ, Lin JP, Wang BB. Journal of the American Chemical Society 2009;131:4564. [PubMed: 19296587]

42. Lee CM, Pai YH, Shieu FS. Journal of the Electrochemical Society 2009;156:B923–B926.

43. Soriaga MP, Hubbard AT. Journal of the American Chemical Society 1982;104:2735–2742.

44. Ssenyange S, Du R, Mcdermott MT. Micro & Nano Letters 2009;4:22–26.

45. Kiema GK, Aktay M, McDermott MT. Journal of Electroanalytical Chemistry 2003;540:7–15.

46. Hermans A, Seipel AT, Miller CE, Wightman RM. Langmuir 2006;22:1964–1969. [PubMed: 16489775]

47. Kolbe H. Annalen der Chemie und Pharmacie 1849;64:339–341.

48. Lund, H.; Hammerich, O. Organic Electrochemistry. 4. M. Dekker; New York: 2001.

49. Tenreiro AM, Nabais C, Correia JP, Fernandes FMSS, Romero JR, Abrantes LM. Journal of Solid State Electrochemistry 2007;11:1059–1069.

50. de Castro CM, Vieira SN, Goncalves RA, Brito-Madurro AG, Madurro JM. Journal of Materials Science 2008;43:475–482.

51. Cooper SE, Venton BJ. Analytical and Bioanalytical Chemistry 2009;394:329–336. [PubMed: 19189084]

52. Pihel K, Hsieh S, Jorgenson JW, Wightman RM. Analytical Chemistry 1995;67:4514–4521. [PubMed: 8633786]
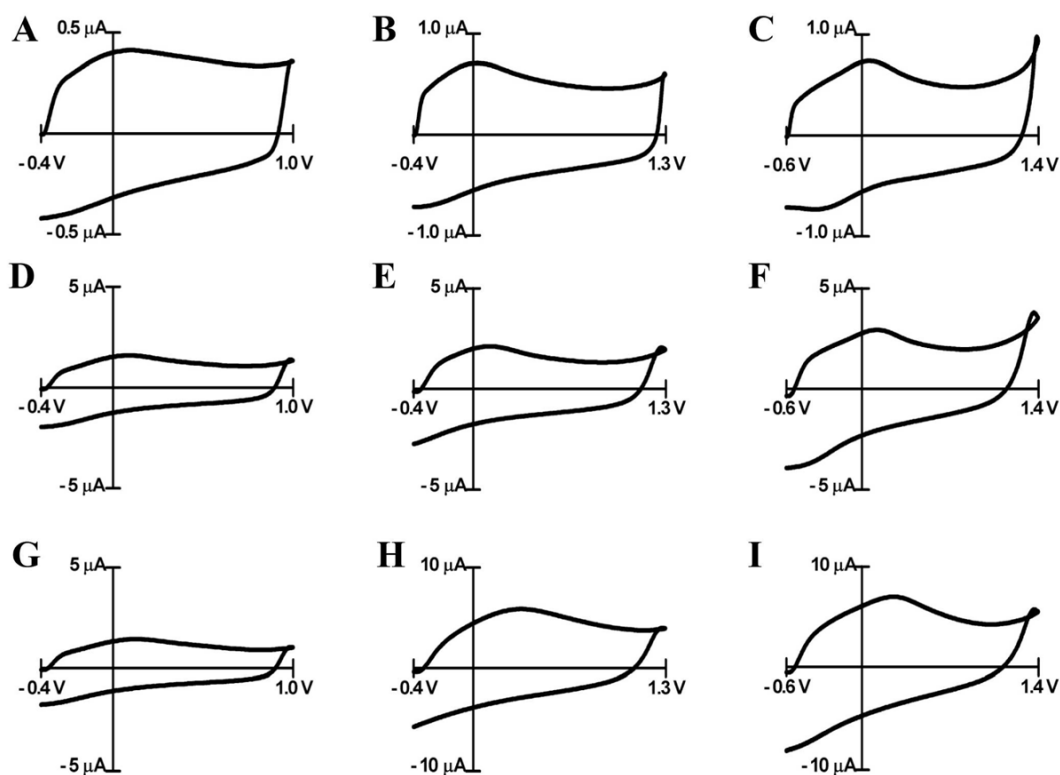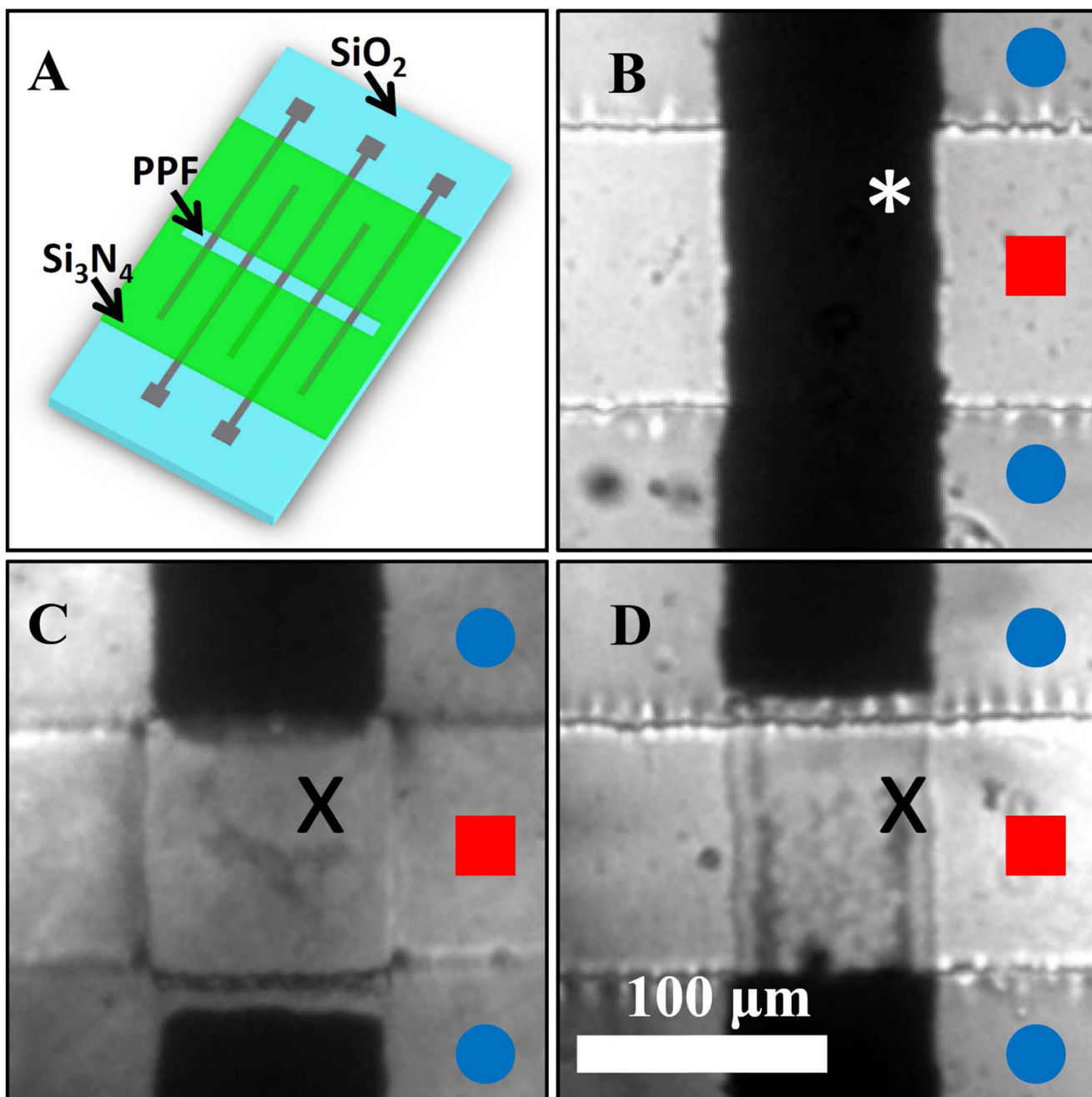
Figure 1.
Cyclic voltammograms in PBS buffer recorded at carbon fiber electrodes (**A–C**) and PPF electrodes (**D–I**). Carbon fiber microelectrodes were cycled at 60 Hz to the potential limits shown for 30 min prior to the recording of these voltammograms. Background currents for PPF electrodes are shown prior to cycling (**D–F**) and at the end (30 min) (**G–I**) of cycling. The anodic potential limits are 1.0 V for **A, D** and **G** (300 V/s), 1.3 V for **B, E** and **H** (400 V/s), and 1.4 V for **C, F** and **I** (400 V/s).
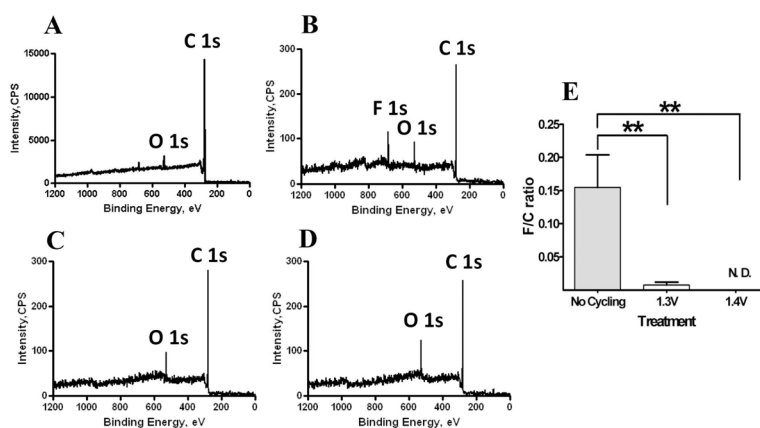
Figure 2.
XPS spectra of PPF electrode surfaces. F 1s, O 1s and C 1s indicate characteristic peaks for fluorine, oxygen and carbon, respectively. (**A**) PPF electrode before any treatment. (**B**) PPF electrode after coating with silicon nitride, removal of insulation by etching with CHF_3/O_2 and subsequent immersion in buffer solution. (**C, D**) PPF electrode after 30 minute treatment with the 1.3 V waveform and the 1.4 V waveform, respectively. Each waveform was repeated at 60 Hz. (**E**) Summary of F/C atomic ratios for PPF electrodes before treatment and after 1.3 V, and 1.4 V treatments. N. D. – no fluorine was detected; double asterisk represents $p < 0.01$ for one way variance ANOVA statistical test (n = 4 for each condition).
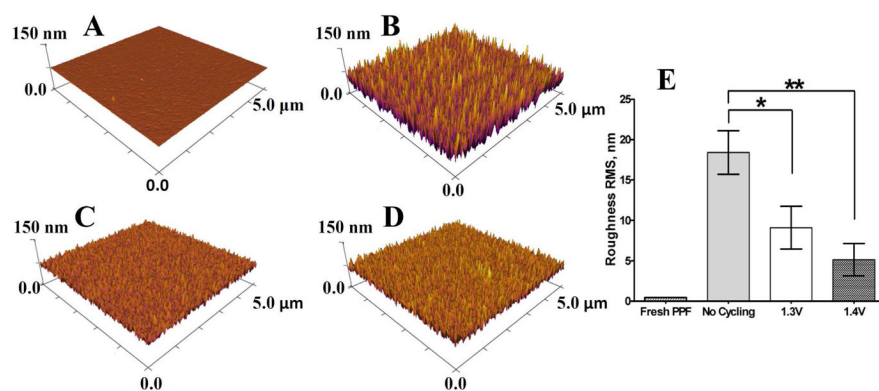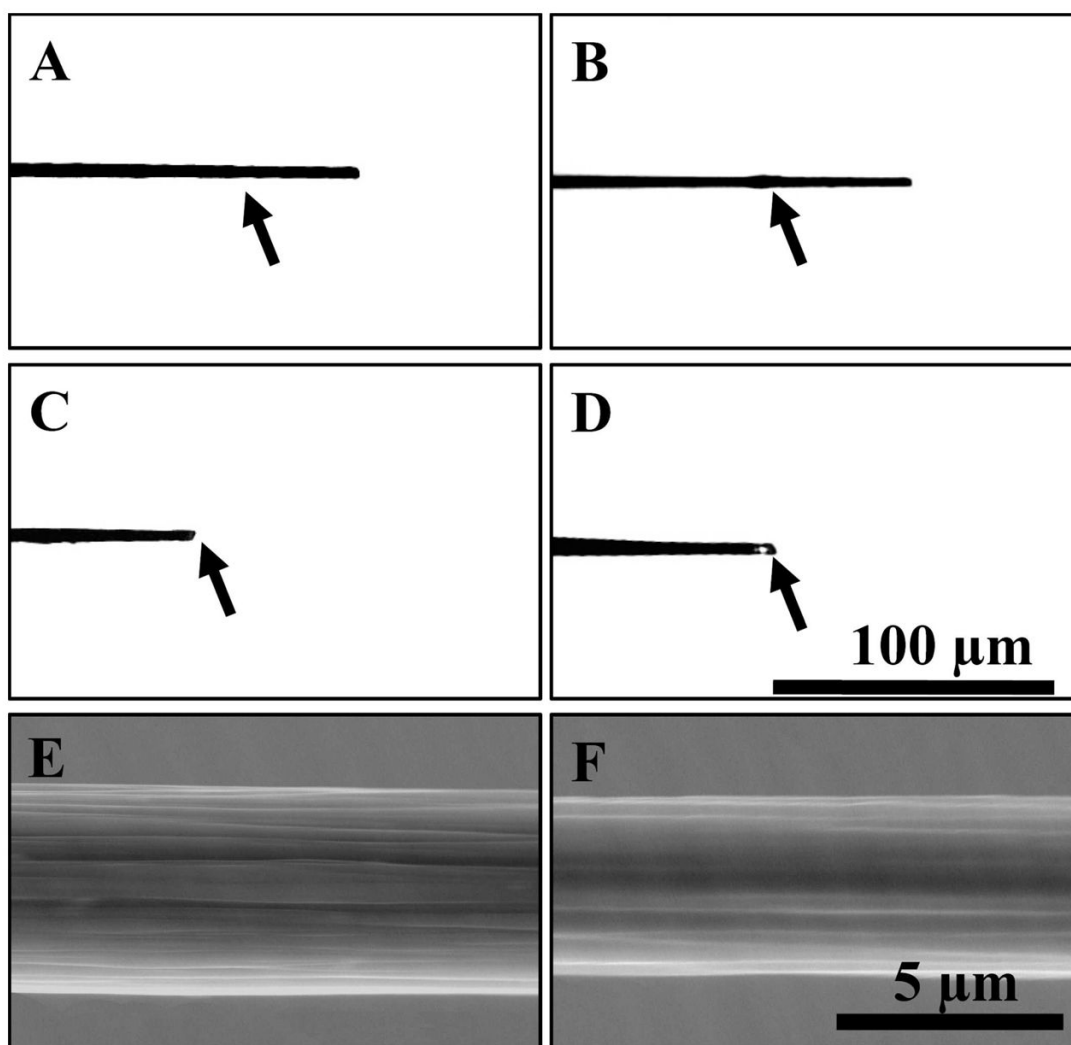
Figure 3.
AFM images of the PPF electrode surface morphology after different treatment conditions. (**A**) PPF electrode before any treatment. (**B**) PPF electrode after coating with silicon nitride, removal of insulation by etching with CHF_3 and subsequent immersion in buffer solution. (**C, D**) PPF electrodes prepared as for (**B**) but following 30 minute treatment with the 1.3 V waveform and the 1.4 V waveform, respectively. Each waveform was repeated at 60 Hz. (**E**) Summary of surface roughness for PPF electrodes before treatment and after 1.3 V, and 1.4 V treatments. Single and double asterisks represent $p < 0.05$ and $p < 0.01$, respectively, for one way variance ANOVA statistical test (n = 3 for each condition).
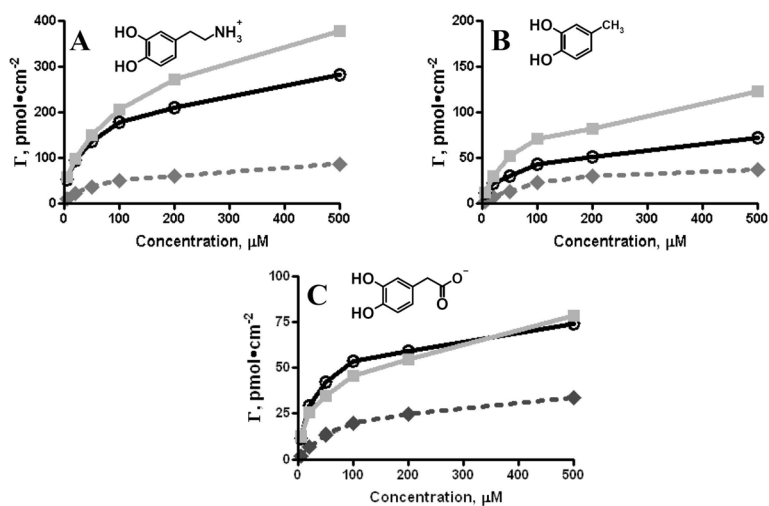
Figure 4.
Images of PPF electrodes after prolonged treatment with the extended waveforms. Optical
microscopy images of PPF electrodes for different electrochemical treatment conditions. (**A**)
schematic of microfabricated chip in which a SiO_2 wafer served as a substrate on which PPF
electrodes were deposited followed by Si_3N_4 insulation. (**B**) PPF electrode immersed in the
buffer before any electrochemical treatment. (**C** and **D**) PPF after 10 hour treatment with the
1.3 V waveform and after 1.5 hour treatment with the 1.4 V waveform, respectively. Blue
circles mark silicon nitride insulation. Red squares mark areas exposed from insulation. A
white asterisk marks the carbon electrode and black Xs mark etched electrodes.
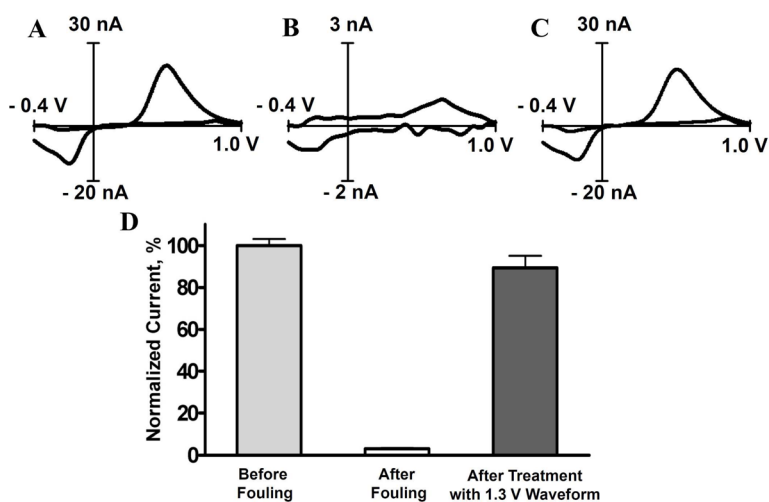
Figure 5.
Images of carbon fiber microelectrodes after prolonged treatment with the extended waveforms. Optical microscopy (**A–D**) and SEM (**E** and **F**) images display the disappearance of the carbon fiber tip after electrochemical etching. The black arrow indicates the location of the end of the glass seal. A carbon fiber microelectrode before treatment (**A**) and after 65 hours (**B**) of treatment with the 1.0 V waveform at 60 Hz. Treatment with the 1.3 V waveform for 65 hours at 60 Hz (**C**) and for 6 hours at 60 Hz with the 1.4 V waveform (**D**) led to the disappearance of the carbon fiber. SEM imaging of T-650 carbon fiber cylinder microelectrodes showed a 0.9 ± 0.4 µm (n = 4) reduction in diameter of the carbon fiber after 30 hr of treatment with the 1.3 V waveform. The same carbon fiber before (**E**) and after (**F**) such treatment.

Figure 6.
Application of the extended waveforms facilitates adsorption of catechols with different functional groups. Adsorption isotherms for the 1.0 V waveform (filled dark grey diamonds), for the 1.3 V waveform (open black circles) and for the 1.4 V waveform (filled grey squares) were obtained by FSCV measurements in a flow injection system. Dopamine (**A**), 4MC (**B**) and DOPAC (**C**) experience increased adsorption for the extended waveforms.

Figure 7.
Sensitivity of a carbon fiber towards 500 nM dopamine fouled by polymerization of tyramine is recovered by brief application of the extended waveform. The sensitivity was monitored with flow injection analysis of 500 nM dopamine. (**A**) A representative background subtracted cyclic voltammogram for dopamine before fouling. (**B**) Electrode fouling by cycling in 15 mM tyramine for 15 minutes almost completely abolishes sensitivity to dopamine. (**C**) The sensitivity of the electrode is completely recovered by cycling for 15 minutes with the 1.3 V waveform. (**D**) Averaged change (n=3) in sensitivity towards dopamine at aforementioned treatment conditions shown as a percent change in cyclic voltammogram peak currents.